

Cite this: *Chem. Sci.*, 2025, **16**, 15734

All publication charges for this article have been paid for by the Royal Society of Chemistry

Received 9th May 2025
Accepted 28th July 2025

DOI: 10.1039/d5sc03359d

rsc.li/chemical-science

Introduction

The synthesis of single-crystal polymers, particularly those with complex topologies such as 2D and 3D structures, remains a significant challenge in the field.^{1–6} In recent years, there have been notable advancements in the solution-phase synthesis of 2D or 3D covalent organic frameworks (COFs) single crystals by using dynamic covalent chemistry, with a few precious examples being characterized by X-ray single-crystal diffraction.^{7–11} The challenge in the synthesis of COF single crystals is the very careful control over the reaction conditions to manage nucleation and crystal growth.^{12–17} Besides the solution-phase synthesis, Schläter pioneered the use of topological polymerization *via* photopolymerization, achieving the first successful preparation of a large-scale 2D polymer single crystal through the solid-phase transformation of a monomer single crystal into a polymer single crystal.¹⁸ The precise structure of this 2D polymer was determined using single-crystal X-ray diffraction (SCXRD). Subsequently, several additional 2D polymer single crystals have been successfully synthesized through photo-irradiated topological polymerization.^{19–21} Recently, Sureshan and co-workers realized a 2D polymer single crystal through the thermally induced topochemical azide–alkyne cycloaddition

reaction.²² Jiang and co-workers achieved successful single-crystal-to-single-crystal (SCSC) transformation by reduction and oxidation of its imine linkages to amine and amide ones.²³ The key challenge in these processes is the precise control of the pre-assembly mode of the monomers during crystallization, achieving the right pattern required for the subsequent polymerization in a single crystal state.^{6,24–28} SCXRD can offer atomic-level structures with unparalleled accuracy. This precise structural information is crucial for understanding the exact topology, connectivity, and symmetry of these framework materials, which are often challenging to characterize in polycrystalline or amorphous samples. However, whether in the solution-phase synthesis of COF single crystals or topological polymerization in a single crystal state, successful synthesis is highly challenging, and examples where the structure has been accurately characterized by SCXRD are extremely rare.

These precious single-crystal examples provide a unique platform to study the mechanisms of covalent bond formation within the framework by observing how monomers assemble and react in a single-crystal state. However, it is worth noting that, to date, there have been no studies on the reversibility of depolymerization of such 2D polymers or 2D COF single crystals back to monomer single crystals, leaving this area of research unexplored. In 2021, we successfully achieved the conversion of a monomer single crystal to a 2D polymer single crystal *via* a [2 + 2] photodimerization reaction, resulting in the formation of a 2D polymer single crystal.²¹ It is well-known that the [2 + 2] photodimerization reaction requires only mild external light irradiation, which minimally affects the single crystal. This helps maintain the quality of the single crystal after

^aState Key Laboratory of Advanced Optical Polymer and Manufacturing Technology, College of Polymer Science and Engineering, Qingdao University of Science and Technology, Qingdao 266042, China. E-mail: hliu@qust.edu.cn; yz@qust.edu.cn; Web: <https://en.yz.qust.edu.cn/>

^bSchool of Chemical Engineering and Technology, Sun Yat-sen University, Zhuhai, Guangdong, 519082, China. E-mail: licheng25@mail.sysu.edu.cn



polymerization, making it suitable for SCXRD.^{29,30} More interestingly, the [2 + 2] photodimerization reaction is thermally reversible, allowing for the ring-opening process to be achieved through heating.^{31–33} Therefore, it is theoretically feasible to revert a 2D polymer single crystal back to its monomer single crystal form by heating. According to the literature, cases of reversible single-crystal transformation involving covalent bond changes are exceedingly rare, with existing reports primarily focusing on small molecules and metal-organic frameworks (MOFs).^{34–38} To date, there have been no reports of reversible SCSC transformations involving the cleavage of covalent bonds between polymers with 2D framework structures and their corresponding monomers. The thermally reversible [2 + 2] photodimerization reaction typically requires high temperatures, which imposes stringent conditions that make it challenging to maintain the single crystal quality necessary for SCXRD. Consequently, the molecular structure, arrangement, and other changes occurring during the thermally reversible transformation process remain unknown.

In this work, we achieved the first thermal conversion from a 2D polymer framework single crystal to its monomer single crystal. The process of covalent bond cleavage induced by high temperatures did not significantly compromise the quality of the single crystal, allowing the structure of the depolymerized monomer single crystal to be fully retained. Interestingly, we observed that, compared to the original monomer single-crystal structure, there were no significant changes in the structure or arrangement of the monomers after two cycles of chemical bond transformation in the single-crystal state. As a result, this process can be fully repeated.

Leveraging this characteristic, we successfully fabricated a crystalline thin-film device that functions as a photo-thermal reversible photolithography material by utilizing the photo-polymerization and thermal depolymerization features of single crystalline 2D framework structures. The mechanism underlying the structural changes is well-defined based on the single crystal transformation. Patterns can be written using light and erased or altered with heat. These materials hold transformative potential in redefining traditional photolithographic processes, making them pivotal in shaping next-generation technologies across electronics, healthcare, and environmental applications.^{31,39–41}

Results and discussion

In our previous work, we successfully synthesized a 2D polymer framework (**T-2DP**) single crystal using a SCSC approach through a [2 + 2] cycloaddition reaction.²¹ Building on this achievement, the present study demonstrates that the cyclobutane ring within the framework can be cleaved upon heating the crystals. This thermal treatment induces a depolymerization process, reverting the polymer structure to its original monomeric (**M1**) single crystal through an SCSC transformation, as illustrated in Fig. 1. Notably, the entire process is carried out in the single-crystal state.

The single crystal of **M1** was readily obtained through recrystallization in a mixture of acetic acid and formic acid (3 : 1

by volume), forming a packing arrangement capable of undergoing [2 + 2] cycloaddition upon irradiation (Fig. 1a). Specifically, the formation of **M1** single crystals involves non-covalent interactions between the solvents (formic acid and acetic acid) and **M1** molecules, along with π - π stacking among **M1** units. These interactions guide the organization into a 2D supramolecular framework, which subsequently undergoes photo-polymerization to form the **T-2DP** single crystal. Solvent molecules act as template-like agents during the assembly of monomer single crystals, influencing both the packing and the resulting framework geometry. Single crystal X-ray crystallography analysis revealed that **M1** crystallizes in the $R\bar{3}$ space group, with cell parameters: $a = 27.2176$ (5) Å, $b = 27.2176$ (5) Å, $c = 16.2768$ (3) Å, $\alpha = 90^\circ$, $\beta = 90^\circ$, $\gamma = 120^\circ$, $V = 10\,442.4$ (4) Å³ (Table S1). The **M1** molecule adopts a head-to-tail arrangement of its three arms, forming a hexagonal structure in a 2D plane along the *a*- and *b*-axis (Fig. 1). Additionally, the distance between adjacent styryl units, measured at 3.919 Å (Fig. 1b), meets Schmidt's criteria for [2 + 2] photocycloaddition, enabling the UV-induced conversion of **M1** into the 2D polymer **T-2DP**.^{42,43}

The **M1** single crystal was then irradiated with 530 nm light for 12 hours. During this process, the crystal underwent a distinct color change from dark yellow to pale yellow, while maintaining its translucency and without noticeable cracks. This realized the polymerization in a single-crystal state and led to the formation of the single-crystal **T-2DP**. **T-2DP** crystal belongs to the $R\bar{3}$ space group with the following cell parameters: $a = 26.6621$ (3) Å, $b = 26.6621$ (3) Å, $c = 16.8900$ (2) Å, $\alpha = 90^\circ$, $\beta = 90^\circ$, $\gamma = 120^\circ$, $V = 10\,398.0$ (3) Å³ (Table S1). The monomer molecules in each layer with the neighboring olefin moieties participate in the formation of the 2D polymer through dimerization of [2 + 2] cycloaddition (Fig. 2a), generating a new covalently connected 2D layer in **T-2DP** (Fig. 2b). The carbon atoms at the reactive sites in the crystal underwent considerable displacement before and after the [2 + 2] cycloaddition reaction. Specifically, the distance of the neighboring olefinic moieties (–C=C–) in the monomer (3.919 Å) decreased to 1.587 Å of the –C–C– bond in the cyclobutene moieties of the 2D polymers with an average displacement of 2.332 Å per reactive carbon atom (Fig. 1b). The lattice volume of the **T-2DP** crystal shrank by only 0.42% compared to the **M1** crystal (from 10 442.4 to 10 398.0 Å³) (Table S1). When observing a single layer along the *c*-axis, pores are visible with sizes of 15.925 Å and 29.523 Å, corresponding to the shortest and longest C–C distances within the same pore, respectively (Fig. 1c). Along the *c*-axis, a perfect ABC stacking mode was observed for **M1** and **T-2DP**. As shown in Fig. 2, the self-assembly mode is exactly the same in the A, B, and C layers except for the periodic staggered shift. The interlayer distance is 3.312 Å in **T-2DP** (Fig. 2b and S2).

The most interesting phenomenon happens in the depolymerization process. It is found that the **T-2DP** single crystal is capable of depolymerizing back to a monomer single crystal upon heating. As early as the 1980s, Hesse and Hünig demonstrated that cyclobutane rings could undergo cycloreversion reactions under heating conditions.⁴⁴ Although the reversible cleavage of cyclobutane rings is well-known in organic systems,



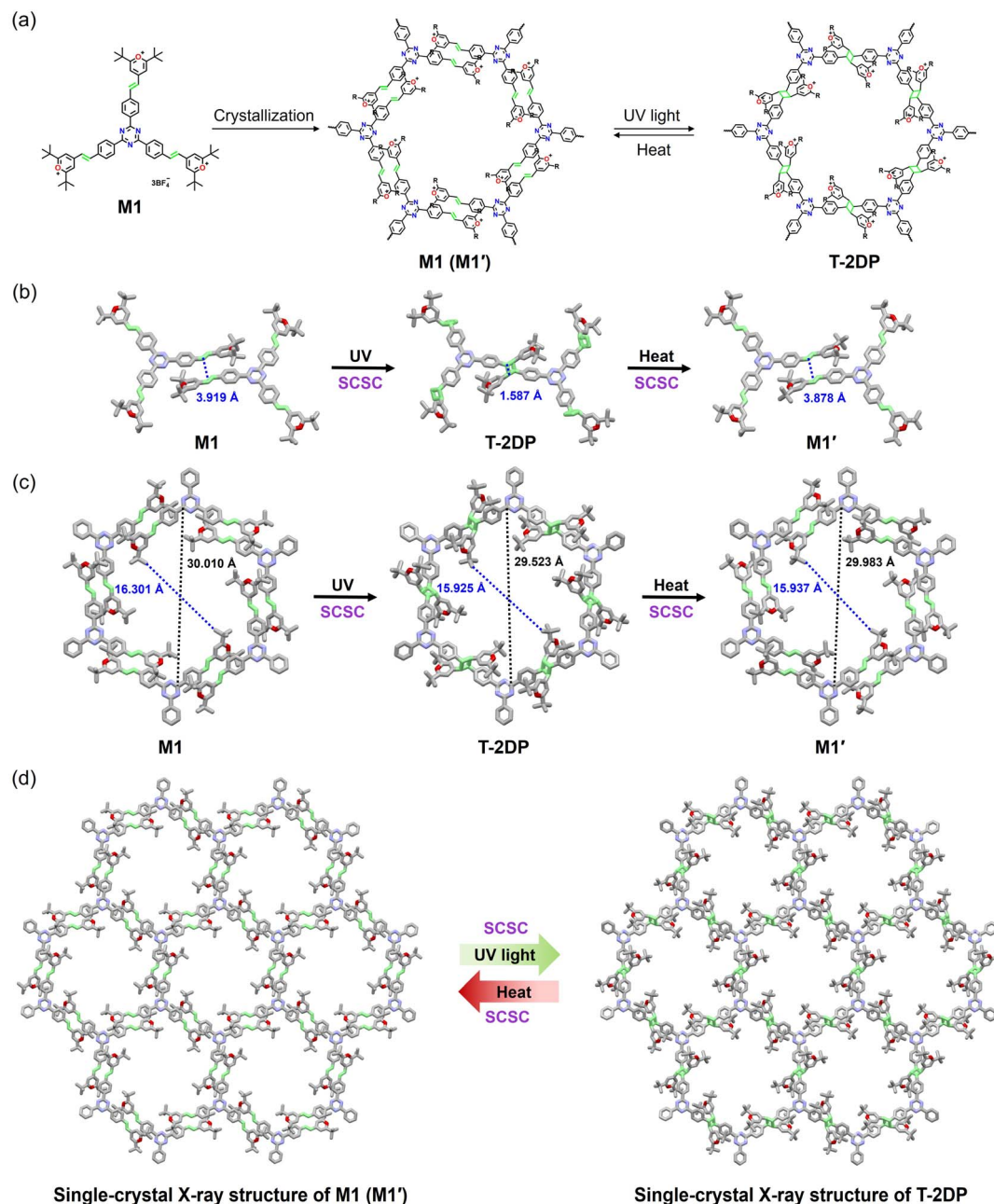


Fig. 1 (a) Chemical structures of monomer **M1**, the pre-organized **M1'** (thermally depolymerized monomer **M1'**) and the 2D polymer framework **T-2DP**. (b) The reversible distance change of the neighboring olefinic moieties ($-C=C-$) in the monomer and the dimerized cyclobutene moieties in single crystal states. (c) The shortest and longest C–C distances within the repeated cavity in the single crystals of **M1**, **T-2DP**, and **M1'**. (d) The single-crystal X-ray structures of **M1** (**M1'**) and **T-2DP** through reversible photodimerization/thermal depolymerization.

no reversible structural transformations have been reported to date in such metal-free 2D polymer framework systems in the SCSC manner.

To determine the depolymerization temperature, differential scanning calorimetry (DSC) was performed on the **T-2DP** single crystal under nitrogen. The DSC data showed an exothermic peak at 236 °C, which aligns with literature reports on the cleavage of cyclobutane rings (Fig. S3).³² Thermogravimetric analysis (TGA) of **T-2DP** and **M1** under an inert atmosphere reveals similar behavior, showing a stable plateau at lower

temperatures followed by a sharp mass loss above 315 °C. This indicates that both **M1** and **T-2DP** maintain stability up to this temperature (Fig. S4).

The **T-2DP** single crystal was subsequently placed in an oven and heated at 240 °C for 30 minutes. During this process, the pale yellow **T-2DP** crystals transformed into brown crystals (designated as **M1'**), exhibiting some cracks (Fig. S1). Fortunately, the single-crystal X-ray analysis data of **M1'** could be collected for a successful refinement. The single crystal structure clearly illustrates the reversible SCSC transformation from

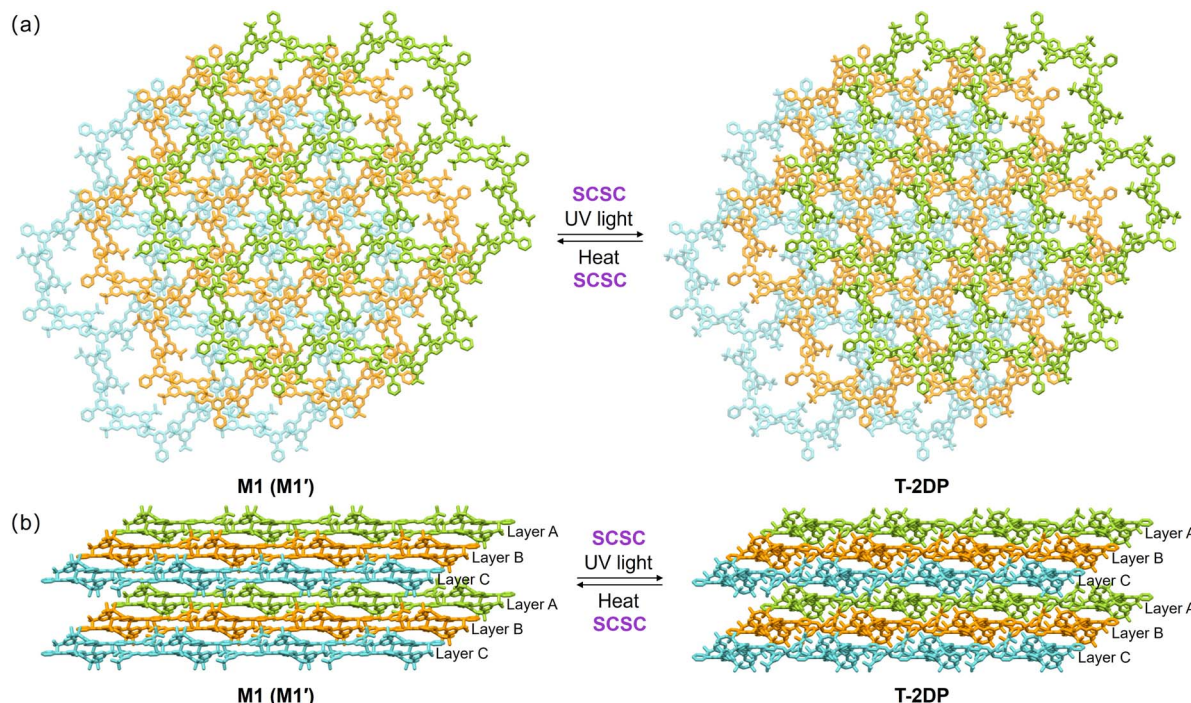


Fig. 2 (a) The three periodic layers of monomer **M1** (**M1'**) and polymer **T-2DP** (viewed along the *c*-axis). (b) The three periodic layers of monomer **M1** (**M1'**) and polymer **T-2DP** (viewed along the *a*-axis).

T-2DP to M1' (Fig. 1 and 2). The structure determination of **M1'** confirmed that the space group and 2D structure were retained. During the thermal depolymerization process, solvent molecules would have completely evaporated from the crystal lattice. Therefore, they should play a negligible role in the SCSC transformation during the thermal depolymerization step. As shown in Fig. 1, the 2D self-assembled structure of **M1'** is similar to that of **M1**. **M1'** crystallizes in the $R\bar{3}$ space group with cell parameters of $a = 27.228$ (3) Å, $b = 27.228$ (3) Å, $c = 15.692$ (4) Å, $\alpha = 90^\circ$, $\beta = 90^\circ$, $\gamma = 120^\circ$, and $V = 10\,075.0$ (3) Å³, which are similar to those of **M1** (Table S1). Furthermore, the volume of the **M1'** crystal lattice shrank by only 3.52% compared to the original **M1** crystal (from 10 442.4 to 10 075.0 Å³) (Table S1). No significant changes were observed in the distance between neighboring olefinic moieties ($-C=C-$) within the 2D layers (Fig. 1b) or the pore size (Fig. 1c). However, the relative motion between adjacent monomers within the same layer is pronounced, accompanied by a decrease in the distance from 2.095 Å to 1.875 Å, representing an approximate reduction of 10.5% (Fig. S2). These results established that cleavage of the cyclobutane ring of **T-2DP** to **M1'** can successfully occur in an SCSC manner. Subsequently, the phase purity was confirmed by PXRD (Fig. S5). The ¹H NMR spectrum of the thermolyzed sample **M1'** matched exactly with that of **M1**, confirming the complete reversibility of the transformation from **T-2DP** back to **M1** (Fig. S6).

The Fourier transform infrared (FT-IR) spectrum reveals that, following UV irradiation of the **M1** single crystal, the stretching vibration peak of $-C=C-$ at 1608 cm⁻¹ and the out-of-plane bending vibration peak of $-C-H$ at 948 cm⁻¹ almost

completely disappear. This indicates that the quantitative polymerization of the **M1** single crystal has been successfully achieved (Fig. 3a and S7). Upon heating **T-2DP**, these peaks reemerge at their original positions, confirming the successful quantitative depolymerization of the polymer crystal to a monomer crystal. Furthermore, **M1'** can undergo quantitative polymerization again upon UV irradiation to generate **T-2DP'**, as clearly evidenced by the FT-IR spectra (Fig. 3a and S7). In addition to the evidence from FT-IR, the UV-vis absorption spectra also reveal that both **M1** and **M1'** exhibit absorption maxima at 412 nm, while this absorption band is absent in **T-2DP** (Fig. 3b). The entire process is visible to the naked eye (Fig. 3c). These results further confirm the reversibility of the reaction between **M1** and **T-2DP**. After the second round of UV irradiation, the transparency and single-crystal nature of the **T-2DP'** crystals were found to be preserved (Fig. S8). These results demonstrate the good reversibility of the single-crystal monomer and the 2D polymer, underscoring the potential of this material as a promising candidate for reversible materials.^{32,37,45}

It is observed that the **M1** molecule exhibits excellent film-forming properties on different substrates. This provides a critical parameter for evaluating its potential applications and performance. A uniform yellow thin film on glass substrates can be easily obtained through the solution spin coating method (Fig. 4). After being exposed to 385 nm UV light for 10 seconds, the yellow color completely disappeared, resulting in a colorless and transparent glass slide. The slide was positioned on a heating plate maintained at 240 °C. Within approximately 60 seconds of heating, the slide exhibited a gradual color change from colorless to pale yellow. This observation indicates the

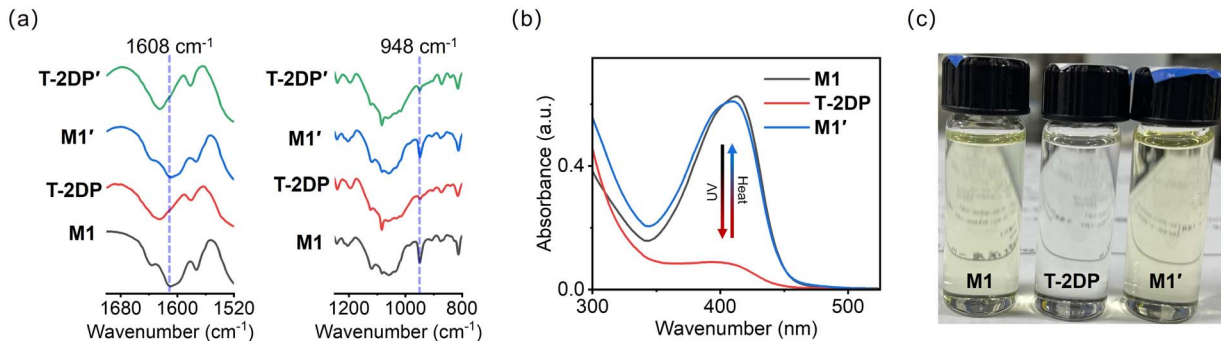


Fig. 3 (a) The FT-IR spectra of M1, T-2DP, M1' and T-2DP'. (b) The UV-vis absorption spectra of M1, T-2DP, and M1' (10^{-5} M in trifluoroacetic acid/1,4-butyrolactone = 3 : 50). (c) The photographs of M1, T-2DP, M1' solution (10^{-5} M in trifluoroacetic acid/1,4-butyrolactone = 3 : 50).

successful depolymerization of T-2DP on the glass, leading to the formation of M1' (Fig. 4a). This phenomenon is consistent with the photopolymerization behavior observed in the single-crystal study. Subsequently, a photomask featuring a “smiley face” pattern was placed over the film, which was then exposed to 385 nm UV light for 10 seconds. Upon removing the photomask, a clear contrast emerged between the exposed and unexposed regions (Fig. 4b). The exposed areas of the film

changed from yellow to colorless, creating a distinct “smiley face” pattern. The glass slide was then thoroughly washed with dichloromethane, during which the unexposed areas dissolved, leaving the slide entirely colorless. Subsequently, the glass slide was placed on a heating plate set to 240 °C for 60 seconds, during which the “smiley face” pattern on the glass was distinctly re-revealed (Fig. 4b). While the unexposed film dissolved within seconds, the “smiley face” remained intact even

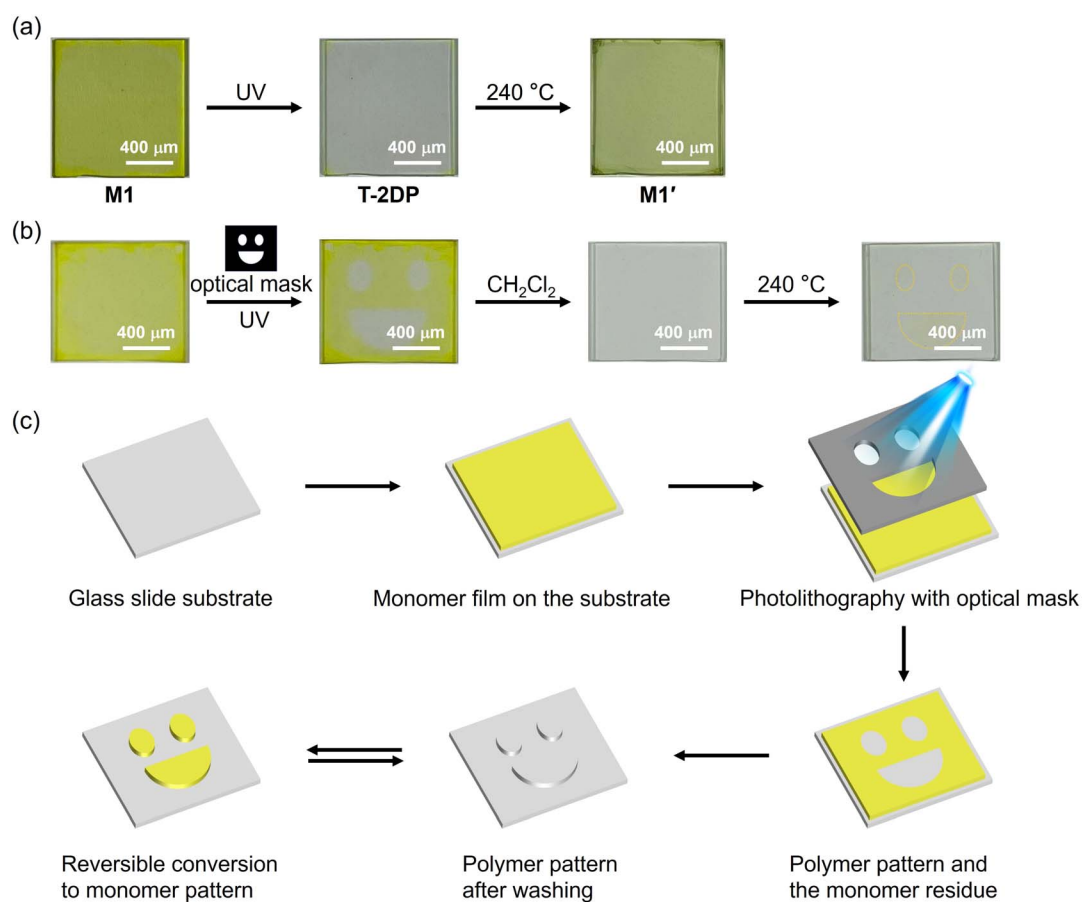


Fig. 4 (a) Photographs of the photo/thermal reversibility behavior of the M1/T-2DP films on the glass slide substrate. (b) Photographs of the photo/thermal reversible photolithography of the M1/T-2DP films on the glass slide substrate. (c) Schematic illustration of the photo/thermal reversible photolithography of the M1/T-2DP film on the glass slide substrate.



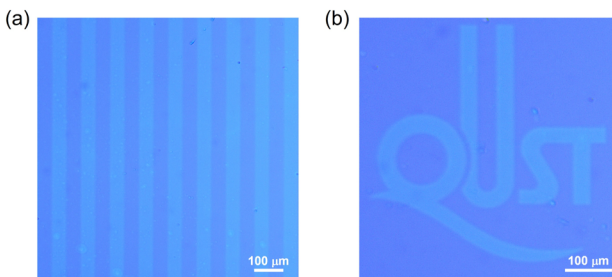


Fig. 5 (a) AFM image of micron stripes from a photoresist of a thin film based on **M1**. (b) AFM image of the patterns of "QUST" from a photoresist of a thin film based on **M1**.

after multiple CH_2Cl_2 washes. This significant reduction in the solubility of the thin film after UV exposure is attributed to the photopolymerization of **M1**, leading to the formation of insoluble polymer **T-2DP**. The sharp features of the pattern and high sensitivity to UV light confirm the applicability of this system as an efficient photolithography material. More interestingly, due to the highly ordered structures of either monomer or polymer on the glass substrate, the reversibility of the films through photo/thermal stimulation can be successfully achieved. This demonstrates that the polymerization and the depolymerization process on the glass slide device can be easily realized through short-time UV irradiation and heating. Thus, an interesting photolithography material with rewritable characteristics was obtained. These unique properties enable dynamic, reconfigurable, or multifunctional devices, making them highly valuable in cutting-edge technology fields.

Subsequently, high-resolution photopatterning was carried out on Si/SiO_2 substrates. A thin film of **M1** was deposited by spin-coating from a saturated chloroform solution, followed by the application of a photomask. Upon irradiation with 365 nm UV light, the film was developed by immersing it in chloroform for 30 seconds, selectively removing the unexposed regions. This process effectively transferred the photomask's transparent patterns onto the **M1** thin film. Various micro-patterns, including well-defined stripes and the letters "QUST," were successfully fabricated using different photomasks. As illustrated in Fig. 5, the resulting patterns exhibit sharp boundaries and high contrast, where the brighter and darker regions correspond to the photoinduced polymerized and unreacted monomer areas, respectively. These observations underscore the excellent pattern fidelity and resolution of **M1** films, validating their potential as efficient photoresists. Taken together, these findings highlight the promise of solid-state [2 + 2] cycloaddition chemistry as a viable and attractive strategy for the development of high-performance photoresist materials.

Conclusions

In this work, the photo/thermal reversible transformation between the single-crystal 2D polymer framework and its monomer was achieved without compromising single-crystal quality, allowing for precise structural characterization through single-crystal X-ray diffraction analysis. Utilizing this

unique reversible ability, we developed a photolithography material with rewritable characteristics. This material allows patterns to be written using UV light and erased or modified with heat, unlocking potential applications in reconfigurable devices for intelligent manufacturing and dynamic micro/nanosystems.

Author contributions

H. Wang carried out all the experiments. C. Sun and X. Jia participated in the synthesis of compound **M1**. H. Liu guided the synthesis process. C. Li conducted high-resolution pattern preparation and guided the process. H. Wang and Y. Zhao co-wrote the manuscript. Y. Zhao directed the whole project.

Conflicts of interest

There are no conflicts to declare.

Data availability

The data supporting this article have been included as part of the SI.

CCDC 2415163 contains the supplementary crystallographic data for this paper.⁴⁶

Experimental procedures and spectroscopic data, including Table S1, Figures S1–S8. See DOI: <https://doi.org/10.1039/d5sc03359d>.

Acknowledgements

Acknowledgments are extended to the National Natural Science Foundation of China (22475115, 22175101 and 22205128) for their valuable financial support. We thank the Shanghai Synchrotron Radiation Facility of BL17B1 (<https://cstr.cn/31124.02.SSRF.BL17B1>) for assistance with single crystal testing measurements.

References

- 1 C. Gropp, T. Ma, N. Hanikel and O. M. Yaghi, Design of Higher Valency in Covalent Organic Frameworks, *Science*, 2020, **370**(6515), eabd6406.
- 2 T. Ma, E. A. Kapustin, S. X. Yin, L. Liang, Z. Zhou, J. Niu, L.-H. Li, Y. Wang, J. Su, J. Li, X. Wang, W. D. Wang, W. Wang, J. Sun and O. M. Yaghi, Single-Crystal X-Ray Diffraction Structures of Covalent Organic Frameworks, *Science*, 2018, **361**(6397), 48–52.
- 3 Z. Zhou, L. Zhang, Y. Yang, I. J. Vitorica-Yrezabal, H. Wang, F. Tan, L. Gong, Y. Li, P. Chen, X. Dong, Z. Liang, J. Yang, C. Wang, Y. Hong, Y. Qiu, A. Gölzhäuser, X. Chen, H. Qi, S. Yang, W. Liu, J. Sun and Z. Zheng, Growth of Single-Crystal Imine-Linked Covalent Organic Frameworks Using Amphiphilic Amino-Acid Derivatives in Water, *Nat. Chem.*, 2023, **15**(6), 841–847.
- 4 S. Li, S. Xu, E. Lin, T. Wang, H. Yang, J. Han, Y. Zhao, Q. Xue, P. Samori, Z. Zhang and T. Zhang, Synthesis of Single-



Crystalline Sp₂-Carbon-Linked Covalent Organic Frameworks through Imine-to-Olefin Transformation, *Nat. Chem.*, 2025, 226–232.

5 A. M. Evans, L. R. Parent, N. C. Flanders, R. P. Bisbey, E. Vitaku, M. S. Kirschner, R. D. Schaller, L. X. Chen, N. C. Gianneschi and W. R. Dichtel, Seeded Growth of Single-Crystal Two-Dimensional Covalent Organic Frameworks, *Science*, 2018, **361**(6397), 52–57.

6 M. Wang, Y. Jin, W. Zhang and Y. Zhao, Single-Crystal Polymers (Sceps): From 1d to 3d Architectures, *Chem. Soc. Rev.*, 2023, **52**(23), 8165–8193.

7 L. Yi, Y. Gao, S. Luo, T. Wang and H. Deng, Structure Evolution of 2d Covalent Organic Frameworks Unveiled by Single-Crystal X-Ray Diffraction, *J. Am. Chem. Soc.*, 2024, **146**(29), 19643–19648.

8 X. Wang, Y. Wada, T. Shimada, A. Kosaka, K. Adachi, D. Hashizume, K. Yazawa, H. Uekusa, Y. Shoji, T. Fukushima, M. Kawano and Y. Murakami, Triple Isomerism in 3d Covalent Organic Frameworks, *J. Am. Chem. Soc.*, 2024, **146**(3), 1832–1838.

9 T. Kitano, S. Goto, X. Wang, T. Kamihara, Y. Sei, Y. Kondo, T. Sannomiya, H. Uekusa and Y. Murakami, 2.5-Dimensional Covalent Organic Frameworks, *Nat. Commun.*, 2025, **16**(1), 280.

10 B. Yu, W. Li, X. Wang, J.-H. Li, R.-B. Lin, H. Wang, X. Ding, Y. Jin, X. Yang, H. Wu, W. Zhou, J. Zhang and J. Jiang, Observation of Interpenetrated Topology Isomerism for Covalent Organic Frameworks with Atom-Resolution Single Crystal Structures, *J. Am. Chem. Soc.*, 2023, **145**(46), 25332–25340.

11 J. Han, J. Feng, J. Kang, J.-M. Chen, X.-Y. Du, S.-Y. Ding, L. Liang and W. Wang, Fast Growth of Single-Crystal Covalent Organic Frameworks for Laboratory X-Ray Diffraction, *Science*, 2024, **383**(6686), 1014–1019.

12 Y. Yin, Y. Zhang, X. Zhou, B. Gui, G. Cai, J. Sun and C. Wang, Single-Crystal Three-Dimensional Covalent Organic Framework Constructed from 6-Connected Triangular Prism Node, *J. Am. Chem. Soc.*, 2023, **145**(41), 22329–22334.

13 Y. Yin, Y. Zhang, X. Zhou, B. Gui, W. Wang, W. Jiang, Y.-B. Zhang, J. Sun and C. Wang, Ultrahigh-Surface Area Covalent Organic Frameworks for Methane Adsorption, *Science*, 2024, **386**(6722), 693–696.

14 J. Zhang, Z. Wang, J. Suo, C. Tuo, F. Chen, J. Chang, H. Zheng, H. Li, D. Zhang, Q. Fang and S. Qiu, Morphological Tuning of Covalent Organic Framework Single Crystals, *J. Am. Chem. Soc.*, 2024, **146**(51), 35090–35097.

15 C. Chen, L. Cao, Y. Liu, Z. Li, Z.-H. Li, G. Zhou, D. Zhang, X. Huang, Y. Wang, G. Li, L. Liu, Y.-Y. Yuan, Y. Zhang, Q. Wang, Y. Chen, Z. Shi, Q. Fang, Z. Huang, Z. Lai and Y. Han, Investigating a Seemingly Simple Imine-Linked Covalent Organic Framework Structure, *J. Am. Chem. Soc.*, 2024, **146**(51), 35504–35512.

16 L. Deng, W. Chen, G. Zhou, Y. Liu, L. Liu, Y. Han, Z. Huang and D. Jiang, Synthesis of Single-Crystal Two-Dimensional Covalent Organic Frameworks and Uncovering Their Hidden Structural Features by Three-Dimensional Electron Diffraction, *J. Am. Chem. Soc.*, 2024, **146**(51), 35427–35437.

17 Z. Zhou, G. Cai, Z. Zhang, G. Li, D. Lou, S. Qu, Y. Li, M. Huang, W. Liu, Z. Zheng and J. Sun, Conformational Chirality of Single-Crystal Covalent Organic Frameworks, *J. Am. Chem. Soc.*, 2024, **146**(49), 34064–34069.

18 M. J. Kory, M. Wörle, T. Weber, P. Payamyr, S. W. van de Poll, J. Dshemuchadse, N. Trapp and A. D. Schlüter, Gram-Scale Synthesis of Two-Dimensional Polymer Crystals and Their Structure Analysis by X-Ray Diffraction, *Nat. Chem.*, 2014, **6**(9), 779–784.

19 R. Z. Lange, G. Hofer, T. Weber and A. D. Schlüter, A Two-Dimensional Polymer Synthesized through Topochemical [2 + 2]-Cycloaddition on the Multigram Scale, *J. Am. Chem. Soc.*, 2017, **139**(5), 2053–2059.

20 R. Bhola, P. Payamyr, D. J. Murray, B. Kumar, A. J. Teator, M. U. Schmidt, S. M. Hammer, A. Saha, J. Sakamoto, A. D. Schlüter and B. T. King, A Two-Dimensional Polymer from the Anthracene Dimer and Triptycene Motifs, *J. Am. Chem. Soc.*, 2013, **135**(38), 14134–14141.

21 F. Hu, W. Hao, D. Mücke, Q. Pan, Z. Li, H. Qi and Y. Zhao, Highly Efficient Preparation of Single-Layer Two-Dimensional Polymer Obtained from Single-Crystal to Single-Crystal Synthesis, *J. Am. Chem. Soc.*, 2021, **143**(15), 5636–5642.

22 H. Balan and K. M. Sureshan, Hierarchical Single-Crystal-to-Single-Crystal Transformations of a Monomer to a 1d-Polymer and Then to a 2d-Polymer, *Nat. Commun.*, 2024, **15**(1), 6638.

23 B. Yu, R.-B. Lin, G. Xu, Z.-H. Fu, H. Wu, W. Zhou, S. Lu, Q.-W. Li, Y. Jin, J.-H. Li, Z. Zhang, H. Wang, Z. Yan, X. Liu, K. Wang, B. Chen and J. Jiang, Linkage Conversions in Single-Crystalline Covalent Organic Frameworks, *Nat. Chem.*, 2024, **16**(1), 114–121.

24 V. Ramamurthy and J. Sivaguru, Supramolecular Photochemistry as a Potential Synthetic Tool: Photocycloaddition, *Chem. Rev.*, 2016, **116**(17), 9914–9993.

25 F. Hu, X. Bi, X. Chen, Q. Pan and Y. Zhao, Single-Crystal-to-Single-Crystal Transformations for the Preparation of Small Molecules, 1d and 2d Polymers Single Crystals, *Chem. Lett.*, 2021, **50**(5), 1015–1029.

26 K. Biradha and R. Santra, Crystal Engineering of Topochemical Solid State Reactions, *Chem. Soc. Rev.*, 2013, **42**(3), 950–967.

27 S.-L. Huang, T. S. A. Hor and G.-X. Jin, Photodriven Single-Crystal-to-Single-Crystal Transformation, *Coord. Chem. Rev.*, 2017, **346**, 112–122.

28 T. Friščić and L. R. MacGillivray, Single-Crystal-to-Single-Crystal [2 + 2] Photodimerizations: From Discovery to Design, *Z. Kristallogr. - Cryst. Mater.*, 2005, **220**(4), 351–363.

29 Q.-H. Guo, M. Jia, Z. Liu, Y. Qiu, H. Chen, D. Shen, X. Zhang, Q. Tu, M. R. Ryder, H. Chen, P. Li, Y. Xu, P. Li, Z. Chen, G. S. Shekhawat, V. P. Dravid, R. Q. Snurr, D. Philp, A. C. H. Sue, O. K. Farha, M. Rolandi and J. F. Stoddart, Single-Crystal Polycationic Polymers Obtained by Single-Crystal-to-Single-Crystal Photopolymerization, *J. Am. Chem. Soc.*, 2020, **142**(13), 6180–6187.



30 Y. Liu, X.-R. Guan, D.-C. Wang, J. F. Stoddart and Q.-H. Guo, Soluble and Processable Single-Crystalline Cationic Polymers, *J. Am. Chem. Soc.*, 2023, **145**(24), 13223–13231.

31 S. Cho, J. Usuba, S. Chakraborty, X. Li and G. G. D. Han, Solid-State Photon Energy Storage Via Reversible [2+2] Cycloaddition of Donor-Acceptor Styrylpyrylium System, *Chem.*, 2023, **9**(11), 3159–3171.

32 J. W. Chung, Y. You, H. S. Huh, B.-K. An, S.-J. Yoon, S. H. Kim, S. W. Lee and S. Y. Park, Shear- and Uv-Induced Fluorescence Switching in Stilbenic Π -Dimer Crystals Powered by Reversible [2 + 2] Cycloaddition, *J. Am. Chem. Soc.*, 2009, **131**(23), 8163–8172.

33 T. Jadhav, Y. Fang, C.-H. Liu, A. Dadvand, E. Hamzehpoor, W. Patterson, A. Jonderian, R. S. Stein and D. F. Perepichka, Transformation between 2d and 3d Covalent Organic Frameworks Via Reversible [2 + 2] Cycloaddition, *J. Am. Chem. Soc.*, 2020, **142**(19), 8862–8870.

34 I.-H. Park, A. Chanthapally, Z. Zhang, S. S. Lee, M. J. Zaworotko and J. J. Vittal, Metal-Organic Organopolymeric Hybrid Framework by Reversible [2+2] Cycloaddition Reaction, *Angew. Chem., Int. Ed.*, 2014, **53**(2), 414–419.

35 I.-H. Park, R. Medishetty, H.-H. Lee, C. E. Mulijanto, H. S. Quah, S. S. Lee and J. J. Vittal, Formation of a Syndiotactic Organic Polymer inside a Mof by a [2+2] Photo-Polymerization Reaction, *Angew. Chem., Int. Ed.*, 2015, **54**(25), 7313–7317.

36 D. A. Sherman, R. Murase, S. G. Duyker, Q. Gu, W. Lewis, T. Lu, Y. Liu and D. M. D'Alessandro, Reversible Single Crystal-to-Single Crystal Double [2+2] Cycloaddition Induces Multifunctional Photo-Mechano-Electrochemical Properties in Framework Materials, *Nat. Commun.*, 2020, **11**(1), 2808.

37 F.-L. Hu, H.-F. Wang, D. Guo, H. Zhang, J.-P. Lang and J. E. Beves, Controlled Formation of Chiral Networks and Their Reversible Chiroptical Switching Behaviour by Uv/Microwave Irradiation, *Chem. Commun.*, 2016, **52**(51), 7990–7993.

38 E. Fernandez-Bartolome, A. Martinez-Martinez, E. Resines-Urien, L. Piñeiro-Lopez and J. S. Costa, Reversible Single-Crystal-to-Single-Crystal Transformations in Coordination Compounds Induced by External Stimuli, *Coord. Chem. Rev.*, 2022, **452**, 214281.

39 T. Chen, I. Amin and R. Jordan, Patterned Polymer Brushes, *Chem. Soc. Rev.*, 2012, **41**(8), 3280–3296.

40 A. del Campo and E. Arzt, Fabrication Approaches for Generating Complex Micro- and Nanopatterns on Polymeric Surfaces, *Chem. Rev.*, 2008, **108**(3), 911–945.

41 M. Irie, T. Fukaminato, T. Sasaki, N. Tamai and T. Kawai, A Digital Fluorescent Molecular Photoswitch, *Nature*, 2002, **420**(6917), 759–760.

42 G. M. J. Schmidt, Photodimerization in the Solid State, *Pure Appl. Chem.*, 1971, **27**(4), 647–678.

43 M. D. Cohen and G. M. J. Schmidt, 383. Topochemistry. Part I. A Survey, *J. Am. Chem. Soc.*, 1964, 1996–2000.

44 K. Hesse and S. Hünig, Mehrstufige Reversible Redoxsysteme, XLIII. Voltammetrie Von α -Styrylpyrylium-Salzen, (1,3-Cyclobutandiy)-Und (1,3-Cyclobutandiyilden) Bis(Pyrylium)-Salzen, *Liebigs Ann. Chem.*, 1985, **1985**(4), 740–750.

45 H. Meier and D. Cao, Optical Switches with Biplanemers Obtained by Intramolecular Photocycloaddition Reactions of Tethered Arenes, *Chem. Soc. Rev.*, 2013, **42**(1), 143–155.

46 H. Wang, C. Sun, X. Jia, H. Liu, C. Li and Y. Zhao, Reversible transformation of single-crystal two-dimensional polymer framework for photo/thermal reversible photolithography (2415163: The crystal structure of M1' was determined at 100 K using a single crystal X-ray diffractometer (Rigaku) at Shandong University), 2025.

